Fraunhofer diffraction from a ring aperture with a spiral phase transmission function: numerical and analytical studies

IVO AUBRECHT, MIROSLAV MILER, JAN PALA

Institute of Radio Engineering and Electronics, Academy of Sciences of the Czech Republic, Chaberská 57, 182 51 Prague 8, Czech Republic, e-mail: aubrecht@ure.cas.cz.

Fraunhofer diffraction patterns from a spiral phase element with an annular aperture are investigated, on normal incidence of a plane monochromatic wave, depending on a spiral distribution of the phase of a wave at the output from the element. Results of extensive numerical calculations are presented and analytical formulas are derived for a very thin aperture. Basic behaviour of diffraction patterns depending on the spiral's slope is predictable from the analytical approximation.

Keywords: spiralphase filters, phase singularities, Fraunhofer diffraction, scalar wave theory.

1. Introduction

Superposition of waves with a smooth wavefront results in a wave whose amplitude can drop to zero locally if destructive interference takes place. At the place of the drop, the phase of the resultant wave is undeterminable. This is an example of a local phase singularity. Assuming elementary spherical waves that propagate from a plane optical element, forming a resultant wave, they have to be conveniently phase shifted with respect to each other for the resultant wave to have the phase singularity. This can be achieved, on normal incidence of a plane wave upon the element, if the element has a spiral phase transmission function.

Such spiral structures have been drawing attention of researchers for about three decades. They have proved to be of use for various practical applications, such as wavefront inspection [1], shifting of light beam frequency [2], scattering reduction in omnidirectional antennae [3], and others [4]. They can also be employed for generation of diffraction-limited beams introduced by DURNIN [5]. In this case, light passes only through a thin ring aperture that is concentric with respect to the centre of the spiral [6]. Various production techniques have been proposed for these elements [7]–[12]. While BAZHENOV *et al.* [7] and HECKENBERG *et al.* [8] employ a synthesized hologram, the spiral phase function is realized via a helical variation of the thickness of a plate in [10]–[12].
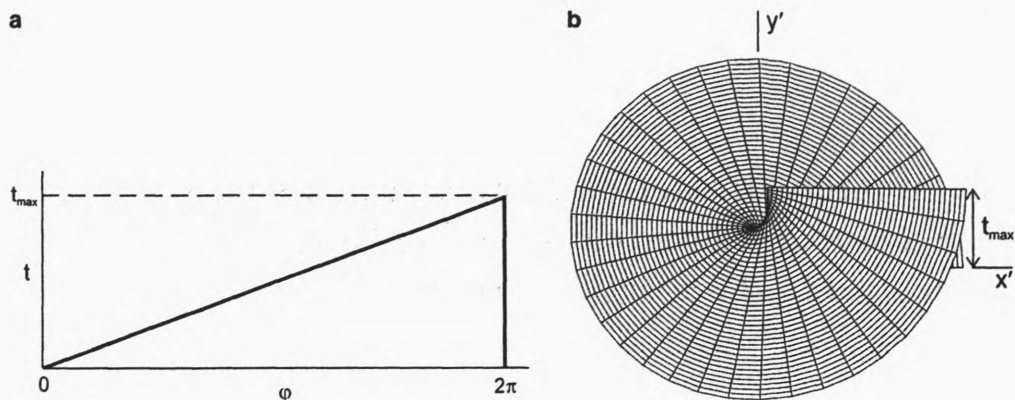
a

b

Fig. 1. Spiral variation of the plate thickness: the thickness as a linear function of the angular coordinate (a), the plot of the plate surface (b).

Consider the latter case. The plate thickness t is a linear function of the angular coordinate φ', as plotted in Fig. 1a, and does not depend on the radial coordinate. The spiral or helical surface of the plate is shown in Fig. 1b. Disregarding a constant phase shift, the phase of the wave passing through the plate acquires the phase increment

$$\Delta\Phi = \frac{2\pi}{\lambda}(n-1)\Delta t \tag{1}$$

with

$$\Delta t = \frac{t_{max} - t_{min}}{2\pi}\varphi' \tag{2}$$

where λ is the wavelength of incident radiation, n is the refractive index of the material the plate is made of, and t_{max} and t_{min} are the maximum and minimum plate thicknesses, respectively. As follows from Eqs. (1) and (2), the phase increment varies with φ' linearly

$$\Delta\Phi = a\varphi', \tag{3}$$

with the slope

$$a = \frac{t_{max} - t_{min}}{\lambda}(n-1). \tag{4}$$

Due to the jump in thickness along the half-line $\varphi = 0$, the phase function of the spiral plate, given by Eq. (1), is discontinuous along this half-line, further referred to as the dislocation half-line.

For the applications mentioned, it is essential that the phase difference between the beginning and the end of the spiral be 2π, or a non-zero integer multiple of 2π. The multiple is just the slope a. During the production of a plate, the slope a increases from

zero until its desired integer value is achieved. The actual value of the slope a can be inferred from the Fraunhofer diffraction pattern generated by the plate. Therefore, it is sensible to investigate the spiral plates with arbitrary values of their slopes, that is, both integer and non-integer ones.

In this paper, we investigate, primarily by numerical methods, the Fraunhofer diffraction pattern from the spiral plate with a ring aperture that is concentric with respect to the centre of the spiral. The reason for this type of aperture is: i) that it is of significance for applications concerning generation of diffraction-limited beams, ii) because primarily the central part is susceptible to production errors, and iii) because this aperture, if thin, allows derivation of relatively simple analytical formulas even for a non-integer a, unlike in [11] where no aperture is considered and the optical field is expressed in terms of Laguerre–Gaussian modes. A property of symmetry of the diffraction pattern is derived, the behaviour of the pattern along the line perpendicular to the dislocation half-line is estimated for a narrow ring aperture, and distributions of intensity at the focal plane of a lens are calculated for the spiral slopes from 0 to 2.

2. Formulation of the problem

The diffraction pattern produced by the spiral phase plate is investigated at the focal plane of a thin condensing lens, as shown in Fig. 2, that is in the Fraunhofer zone. The plate is masked by a ring aperture. Using the paraxial scalar approximation, the optical field at the focal plane is given by

$$u(r, \varphi) = \frac{\exp(ik\psi)}{i\lambda f} \int\limits_{0}^{2\pi} \int\limits_{R_0 - \frac{\Delta R}{2}}^{R_0 + \frac{\Delta R}{2}} u_0(\varphi') \exp\left(-ik\frac{rr'}{f}\cos(\varphi - \varphi')\right) r' dr' d\varphi' \tag{5}$$
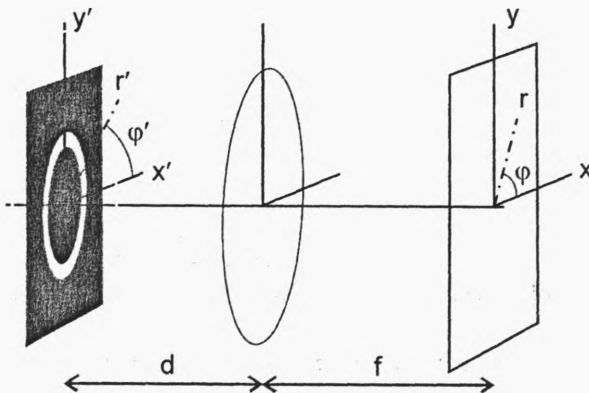

Fig. 2. Scheme of investigation of the diffraction pattern from the spiral phase plate at the focal plane of a thin condensing lens.

where

$$\psi = d + f + \left(1 - \frac{d}{f}\right)\frac{r^2}{2f},$$

while f is the focal distance, d – the distance between the plate and the lens, R_0 and ΔR are the central radius and the width of the ring, r, φ and r', φ' – the polar coordinates at the focal plane and the plate's plane, respectively. The angles are measured counterclockwise with respect to the horizontal axis. The field at the plate's plane $u_0(\varphi')$, is a periodic function, whose period is 2π, with

$$u_0(\varphi') = \exp(ia\varphi') \quad \text{for} \quad 0 < \varphi' < 2\pi. \tag{6}$$

This field arises when a perpendicularly incident plane wave passes through the spiral plate shown in Fig. 1. It can be expanded into the Fourier series

$$u_0(\varphi') = \sum_{l=-\infty}^{\infty} \exp[i(a-l)\pi]\,\text{sinc}(a-l)\,\exp(il\varphi'). \tag{7}$$

Here and throughout the paper, sinc is an abbreviation for the function defined as follows:

$$\text{sinc}\,\xi = \frac{\sin\pi\xi}{\pi\xi}.$$

3. Angular dependence, property of symmetry and axial behaviour

If the slope $a = n$, an integer, then the integral with respect to φ' in Eq. (5) can be expressed in terms of the n-th order Bessel function of the first kind, and the optical field is given by the relation

$$u(r, \varphi) = 2\pi\,\frac{\exp(ik\psi)}{i\lambda f}\,\exp\left[in\left(\varphi - \frac{\pi}{2}\right)\right]\int_{R_0 - \frac{\Delta R}{2}}^{R_0 + \frac{\Delta R}{2}} J_n\left(k\frac{rr'}{f}r'\right)dr'. \tag{8}$$

As the integral in Eq. (8) is not a function of the angular coordinate φ, and the magnitude of the φ-dependent factor before the integral is unity, the intensity of the optical field is independent of φ.

If the slope a is a non-integer, the field at the plate's plane is not a purely harmonic function of φ but a sum of a number of harmonic contributions, as follows from the

Fourier expansion (7) of optical field u_0. Then, the optical field at the focal plane is given by a sum of terms proportional to the right-hand side of Eq. (8)[*]

$$u(r, \varphi) =$$

$$= 2\pi \frac{\exp(ik\psi)}{i\lambda f} \sum_{l=-\infty}^{\infty} \exp[i(a-l)\pi] \operatorname{sinc}(a-l) \exp\left[il\left(\varphi - \frac{\pi}{2}\right)\right] \int_{R_0 - \frac{\Delta R}{2}}^{R_0 + \frac{\Delta R}{2}} J_l\left(k\frac{rr'}{f}r'\right)dr'. \tag{9}$$

Consequently, the intensity becomes dependent on φ, the angular coordinate.

Combining Eqs. (5) and (6), for an arbitrary value of a, it is straightforward to prove that

$$|u(r, \varphi)|^2 = |u(r, \pi - \varphi)|^2. \tag{10}$$

This implies the distribution of intensity at the focal plane to be symmetrical with respect to the line that is perpendicular to the dislocation half-line and that intersects the half-line at centre of the spiral. This symmetry also follows directly from an expansion of the diffraction field under study in terms of Laguerre–Gaussian modes [11].

Another obvious feature is the variation of the optical field with the slope a at the optical axis ($r = 0$)

$$u(0, \varphi) = 2\pi \frac{\exp(ik\psi)}{i\lambda f} \exp(ia\pi) R_0\Delta R \operatorname{sinc}(a). \tag{11}$$

4. Approximate approach

If the apertural ring is thin, that is $\Delta R \ll R_0$, then Eq. (5) simplifies to[**]

$$u(r, \varphi) = \frac{\exp(ik\psi)}{i\lambda f} R_0\Delta R \int_0^{2\pi} \exp(ia\varphi')\exp\left[-ik\frac{rR_0}{f}\cos(\varphi - \varphi')\right]d\varphi'. \tag{12}$$

---

[*]Note that for the calculation of the field at the optical axis, the series (9) has to be summed up first for a nonzero value of r, and then the limiting value of the sum for $r \to 0$ is determined.

[**]Note that a similar expression can be derived also for the field at a distance z from the plate

$$u(r, \varphi;z) = \frac{\exp\left[ik\left(z + \frac{r^2 + R_0^2}{2z}\right)\right]}{i\lambda z} R_0\Delta R \int_0^{2\pi} \exp(ia\varphi')\exp\left[-ik\frac{rR_0}{z}\cos(\varphi - \varphi')\right]d\varphi'.$$

As can be expected from the property of symmetry derived earlier, the behaviour of the pattern along that line of symmetry should be of significance. We have to distinguish between two cases: above the dislocation half-line $\varphi = \pi/2$, and under it, $\varphi = 3\pi/2$.

As noted previously, the axial value of the optical field varies as the sinc function of the argument a, see Eq. (11). What can one infer from this axial behaviour as regards the variation of the diffraction pattern along the line of symmetry? One can expect that when a varies between two neighbouring integers, the whole diffraction pattern gradually shifts. To support this hypothesis, it is convenient to employ an asymptotic expansion of Eq. (12).

Pattern along the line of symmetry above the dislocation half-line. In this case, Eq. (12) can be rewritten to the form

$$u(r, \varphi) = 2\pi \frac{\exp(ik\psi)}{i\lambda f} R_0 \Delta R \exp(ia\pi) \mathbf{J}_a\left(-k\frac{rR_0}{f}\right) \tag{13}$$

where $\mathbf{J}_a$ is Anger's function [13].

Using the property $\mathbf{J}_a(-\xi) = \mathbf{J}_{-a}(\xi)$ and the asymptotic formula for $\mathbf{J}_{-a}(|\xi|)$ [14]

$$\mathbf{J}_{-a} \to \sqrt{\frac{2}{\pi|\xi|}} \cos\left(|\xi| + \frac{a}{2}\pi - \frac{1}{4}\pi\right)$$

Eq. (13) simplifies to

$$u(r, \varphi) = 2\pi \frac{\exp(ik\psi)}{i\lambda f} R_0 \Delta R \exp(ia\pi) \sqrt{\frac{2f}{\pi k r R_0}} \cos\left(k\frac{rR_0}{f} + \frac{a}{2}\pi - \frac{1}{4}\pi\right). \tag{14}$$

Pattern along the line of symmetry under the dislocation half-line. The optical field is expressed by the relation

$$u(r, \varphi) = 2\pi \frac{\exp(ik\psi)}{i\lambda f} R_0 \Delta R \exp(ia\pi) \mathbf{J}_a\left(k\frac{rR_0}{f}\right), \tag{15}$$

and its asymptotic expansion as

$$u(r, \varphi) = 2\pi \frac{\exp(ik\psi)}{i\lambda f} R_0 \Delta R \exp(ia\pi) \sqrt{\frac{2f}{\pi k r R_0}} \cos\left(k\frac{rR_0}{f} - \frac{a}{2}\pi - \frac{1}{4}\pi\right). \tag{16}$$

Comparing Eqs. (14) and (16), we can see that a is with the plus sign in the argument of the cosine function of the first expansion, while a is with the minus sign in the second expansion. This simple fact has a significant consequence. With an increase of a from zero, the diffraction pattern or more exactly its maxima and minima shift down the line of symmetry. This is also obvious from Fig. 3 where variation of the field amplitude along the line of symmetry is shown for the slope a from 0 to 2.
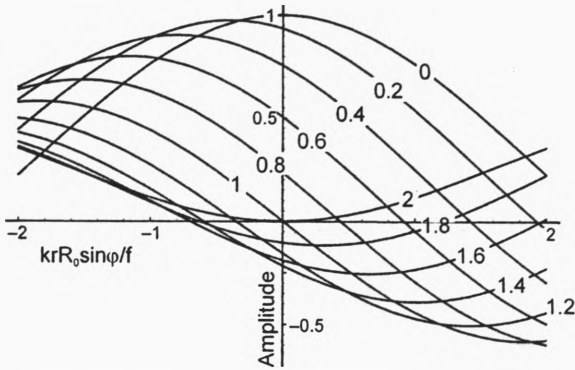
Fig. 3. Variations of the field amplitude along the line of symmetry. The numbers at the curves denote the corresponding values of the slope a.

Finally, we should try to give an answer to the question whether the Eq. (12) can be expressed by means of well-known mathematical functions. For this purpose, we express the second exponential function as a product of two exponential functions, namely

$$\exp\left[-ik\frac{rR_0}{f}\cos(\varphi-\varphi')\right] = \exp\left[-ik\frac{rR_0}{f}\cos\varphi\cos\varphi'\right] \times \exp\left[-ik\frac{rR_0}{f}\sin\varphi\sin\varphi'\right]. \tag{17}$$

The first term of the product can be expanded into the Fourier series

$$\exp\left[-ik\frac{rR_0}{f}\cos\varphi\cos\varphi'\right] = \sum_{l=-\infty}^{\infty}\exp\left(\frac{-il\pi}{2}\right)J_l\left(\frac{rR_0}{f}\cos\varphi\right)\exp(il\varphi'). \tag{18}$$

Combining Eqs. (12), (17) and (18), we arrive at

$$u(r,\varphi) = 2\pi\frac{\exp(ik\psi)}{i\lambda f}R_0\Delta R\exp(ia\pi)\sum_{l=-\infty}^{\infty}\exp\left(\frac{il\pi}{2}\right)J_l\left(\frac{rR_0}{f}\cos\varphi\right)J_{a+l}\left(-\frac{rR_0}{f}\sin\varphi\right). \tag{19}$$

5. Numerical approach

As the optical field u_0 is independent of r' the integral with respect to r' in Eq. (5) can be evaluated by means of elementary integration techniques, and only the integral with respect to φ' remains to be calculated.

The expression for the optical field

$$u(r, \varphi) = \frac{\exp(ik\psi)}{\lambda f} R_0^2 \int\limits_0^{2\pi} \sigma^{-1}\{[(1 + \varepsilon - i\sigma^{-1})\exp(-i(1 + \varepsilon)\sigma)]$$

$$- [(1 - \varepsilon - i\sigma^{-1})\exp(-i(1 + \varepsilon)\sigma)]\} \exp(ia\varphi')\,d\varphi' \qquad (20)$$
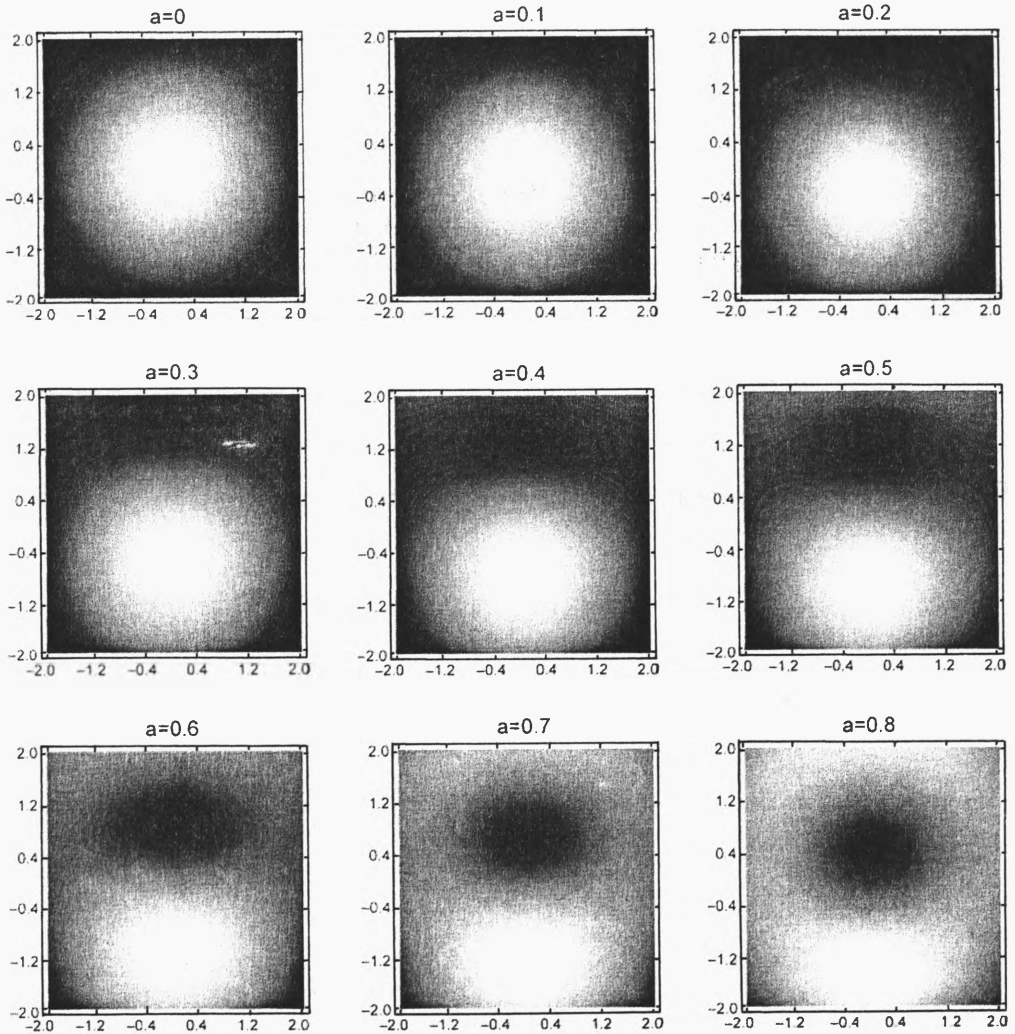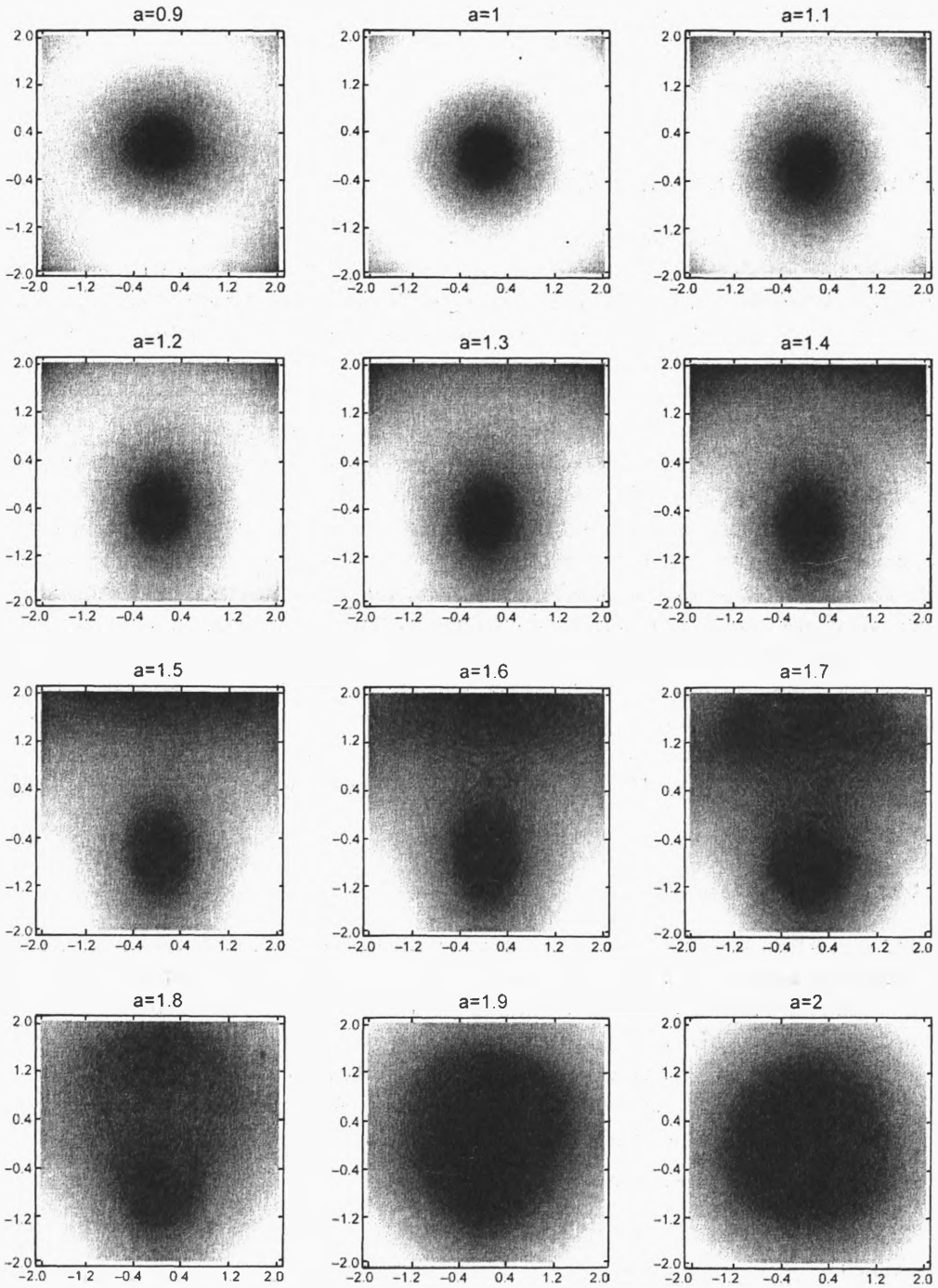

Fig. 4. To be continued.

Fig. 4. Contour plots of the Fraunhofer diffraction pattern for the slope *a* from 0 to 2.

is used for numerical calculations. Here,

$$\sigma = k \frac{rR_0}{f} \cos(\varphi - \varphi'), \quad \varepsilon = \frac{\Delta R}{2R_0}.$$

6. Numerical results and discussion

The variation of the Fraunhofer diffraction pattern from the spiral plate, illuminated by a normally incident coherent plane wave, with the spiral slope is shown by a set of intensity contour plots in Fig. 4. Here $\varepsilon = 0.1$ or $\Delta R = 0.2R_0$. The spiral slope varies from 0 to 2. The unit of the coordinates in the plots is krR_0/f. The plotted values are values of the intensity normalized to the maximum intensity in the area investigated for each particular value of the slope a. They are represented by grey levels, with the black and white levels corresponding to zero and one, respectively. The maximum values of the intensity decrease with the increase of the slope a. For example, the maxima for $a = 0$ and $a = 2$ differ by about a factor of 5.

As can be seen from the set, the diffraction pattern loses radial symmetry when the slope a differs from an integer, in agreement with Sec. (3). The pattern is symmetric with respect to the vertical line. While the slope a increases from zero, the pattern tends to deform and shifts down the line of symmetry. When the slope a approaches unity, the pattern becomes more and more radially symmetric. With further increase of the slope a, the diffraction pattern, again, loses its radial symmetry, and shifts down until the radially symmetric pattern for $a = 2$ is obtained. As regards the axial intensity, it is nonzero only when a differs from 1 and 2, as predicted in Sec. (3).

It can be concluded that the predictions of the approximate model in Sec. (4) prove to be correct.

7. Conclusions

Fraunhofer diffraction patterns from a spiral phase element with an annular aperture are studied within the frame of the scalar wave theory. Attention is paid to the role of the parameter a, the slope of the variation of the phase at the output from the element with the angular coordinate. Extensive numerical results are presented for the slope a varying from 0 to 2. In the case of a thin aperture, analytical formulas for the diffraction field are derived. Basic tendencies in the shape of the diffraction pattern can be predicted from the behaviour of the field along the line of symmetry of the pattern.

References

[1] BRYNGDAHL O., J. Opt. Soc. Am. **63** (1973), 1098.
[2] COURTAL J., DHOLAKIA K., ROBERTSON D.A., ALLEN L., PADGETT M.J., Phys. Rev. Lett. **80** (1998) 3217.
[3] ROBERTSON D.A., MAY P.B., *Omnidirectional Antenna*, UK Patent GB2324659A (1998).

[4]   SOSKIN M.S., VASNETSONV M.V., Prog. Opt. **42** (2001), 219.

[5]   DURNIN J., J. Opt. Soc. Am. A **4** (1973), 651.

[6]   DURNIN J., MICELI J. JR., EBERLY J., Phys. Rev. **58** (1987), 1499.

[7]   BAZHENOV V.YU., VASNETSOV M.V., SOSKIN M.S., JETP Lett. **52** (1990), 429.

[8]   HECKENBERG N.R., MCDUFF R., SMITH C.P., WHITE A.G., Opt. Lett. **17** (1992), 221.

[9]   HECKENBERG N.R., MCDUFF R., SMITH C.P., RUBINSZTEIN-DUNLOP H., WEGENER M.J., Opt. Quantum Electron. **24** (1992), 951.

[10] KHONINA S.N., KOTLYAR V.V., SHINKAREV M.V., SOIFER V.A., USPLENIEV G.V., J. Modern Opt. **39** (1992), 1147.

[11] BEIJERSBERGEN M.W., COERWINKEL R.P.C., KRISTIENSEN M., WOEDERMAN J.P., Opt. Commun. **112** (1994), 321.

[12] BEIJERSBERGEN M.W., *Phase singularities in optical beams*, Ph.D. Thesis, Leiden University, 1996.

[13] ABRAMOWITZ M., STEGUN I.A. [Eds.], *Handbook of Mathematical Functions*, 10th ed., Dover Publications, Inc., New York 1972, p. 498.

[14] WATSON G.N., *Treatise on the Theory of Bessel Functions*, 2nd ed., Cambridge University Press, Cambridge 1958, p. 315 and 199.